mTORC1 promotes survival through translational control of Mcl-1

John R. Mills*, Yoshitaka Hippo[†], Francis Robert*, Samuel M. H. Chen*, Abba Malina*, Chen-Ju Lin*, Ulrike Trojahn*, Hans-Guido Wendel[†‡], Al Charest[§], Roderick T. Bronson[¶], Scott C. Kogan[‖], Robert Nadon**, David E. Housman[†††‡‡], Scott W. Lowe[†§§], and Jerry Pelletier*[‡‡¶¶]

*Department of Biochemistry, [¶¶]McGill Cancer Centre, and **McGill University and Genome Quebec Innovation Centre, McGill University, Montreal, QC, Canada H3G 1Y6; [†]Cold Spring Harbor Laboratory and [§§]Howard Hughes Medical Institute, Cold Spring Harbor, NY 11724; [‡]Department of Cancer Biology and Genetics, Memorial Sloan–Kettering, New York, NY 10021; [§]Molecular Oncology Research Institute, 750 Washington Street, Tufts–New England Medical Center, Box 5609, Boston, MA 02111; [¶]Department of Pathology, Tufts University School of Medicine and Veterinary Medicine, Boston, MA 02111; [‖]Department of Laboratory Medicine, University of California, San Francisco, CA 94143; and [††]Department of Biology and Center for Cancer Research, Massachusetts Institute of Technology, Cambridge, MA 02139

Contributed by David E. Housman, May 18, 2008 (sent for review May 6, 2008)

Activation of the phosphatidylinositol 3-kinase (PI3K)/AKT signaling pathway is a frequent occurrence in human cancers and a major promoter of chemotherapeutic resistance. Inhibition of one downstream target in this pathway, mTORC1, has shown potential to improve chemosensitivity. However, the mechanisms and genetic modifications that confer sensitivity to mTORC1 inhibitors remain unclear. Here, we demonstrate that loss of TSC2 in the *Eμ-myc* murine lymphoma model leads to mTORC1 activation and accelerated oncogenesis caused by a defective apoptotic program despite compromised AKT phosphorylation. Tumors from *Tsc2*$^{+/-}$*Eμ-Myc* mice underwent rapid apoptosis upon blockade of mTORC1 by rapamycin. We identified myeloid cell leukemia sequence 1 (*Mcl-1*), a *bcl-2* like family member, as a translationally regulated genetic determinant of mTORC1-dependent survival. Our results indicate that the extent by which rapamycin can modulate expression of *Mcl-1* is an important feature of the rapamycin response.

rapamycin response | Tsc2 loss | apoptosis | lymphoma | Akt

An important consequence of phosphatidylinositol 3-kinase (PI3K)/AKT pathway activation is stimulation of mammalian target of rapamycin (mTOR), which is associated with altered cell growth, cell survival, and therapeutic response. AKT signaling leads to disruption of the tuberous sclerosis complex [composed of two gene products TSC1 (Harmartin) and TSC2 (Tuberin)] that in turn no longer attenuates RHEB-GTPase activity and results in mTOR activation. There are two structurally distinct mTOR signaling complexes in mammalian cells: the mTOR complex 1 (mTORC1) and mTORC2 (1). One well characterized function of mTORC1 is to maintain protein synthesis in homeostasis with the cellular environment. It achieves this through phosphorylation of at least two direct targets, eukaryotic initiation factor (eIF) 4E-binding proteins (4E-BPs) and ribosomal protein S6 kinases (S6Ks) (2). 4E-BPs bind to and prevent eIF4E from entering into eIF4F, a heterotrimeric complex required for the cap-dependent ribosome recruitment phase of translation initiation. S6K also regulates translation initiation by controlling the activity of eIF4A, a DEAD box RNA helicase, essential to eIF4F function (3).

Rapamycin (*Rap*), an mTOR inhibitor, is currently being investigated as a therapy against numerous cancers (4). It targets primarily mTORC1, although in some cell types, long-term exposure to *Rap* interferes with mTORC2 activity, presumably by sequestering newly synthesized mTOR and reducing nascent mTORC2 complex formation (5). Although many cancers show elevated mTORC1 activity, treatment with *Rap* (or its analogs) is only effective against a subset of tumors (4). Identifying determinants of *Rap* sensitivity is therefore critical to understanding when mTOR inhibition could be an effective cancer therapy. Two proposed mediators of the *Rap* response are: (*i*) the ability of rapamycin to reactivate AKT signaling, normally suppressed by S6K1 (6), and (*ii*) elevated levels of eIF4E (7, 8), although the targets directly mediating sensitivity remain unknown.

In this work, we use a preclinical mouse model to investigate the effect of mTORC1 activation (via TSC2 loss) on translation initiation, oncogenesis, and tumor chemosensitivity. We find that *Tsc2*$^{+/-}$*Eμ-Myc* mice developed aggressive drug-resistant lymphomas that depended on mTORC1 activity for survival. We demonstrate that myeloid leukemia cell sequence 1 (*Mcl-1*), an important antiapoptotic regulator required for the maintenance of mature lymphocytes, is translationally regulated by mTORC1.

Results

Loss of TSC2 Accelerates MYC-Induced Lymphomagenesis. In the *Eμ-myc* mouse tumors model, activation of AKT signaling leads to accelerated tumorigenesis and drug resistance (8). Loss of AKT signaling inhibits cell proliferation and oncogenesis, an effect that can be rescued by hyperactivation of mTORC1, suggesting that AKT may mediate its oncogenic effects exclusively through mTORC1 (9). We therefore sought to determine whether a genetic lesion downstream of AKT, and capable of activating mTORC1, could accelerate lymphomagenesis and drug resistance *in vivo*. Because inactivation of TSC fulfills these requirements (10), we crossed *Tsc2*$^{+/-}$ mice to *Eu-Myc* transgenic mice. *Eμ-Myc* mice developed tumors with a mean onset time of 114 days (Fig. 1*A*) (8, 11). *Tsc2*$^{+/-}$ mice did not develop any lymphoid hyperplasia over the course of this work. In contrast, *Tsc2*$^{+/-}$*Eμ-Myc* mice developed tumors at a significantly accelerated rate (Fig. 1*A*, mean onset time is 47 days, $P < 0.001$). We found that the majority (66%) of tumors from *Tsc2*$^{+/-}$*Eμ-Myc* mice had lost the remaining wild-type *Tsc2* allele (Fig. 1*B*), an event also confirmed by immunoblotting (J.R.M., unpublished observations). Tumors from *Tsc2*$^{+/-}$*Eμ-Myc* mice did not infiltrate the visceral organs as aggressively as *Akt*-driven *Eμ-Myc* tumors (8). They did, however, show a propensity to invade the subarachnoid space of the brain, often accumulating in blood vessels of the cerebellum where they induced infarction leading to overt motor control defects [supporting information (SI) Fig. S1]. Thus, loss of TSC2 greatly accelerated the onset and severity of myc-driven lymphomas.

mTORC1 signaling was activated in primary *Tsc2*$^{+/-}$*Eμ-Myc* tumors that underwent loss of heterozygosity (LOH; referred to in

Author contributions: J.R.M., Y.H., F.R., and J.P. designed research; J.R.M., Y.H., F.R., S.M.H.C., A.M., C.-J.L., U.T., A.C., and S.C.K. performed research; C.-J.L., H.-G.W., and D.E.H. contributed new reagents/analytic tools; J.R.M., Y.H., F.R., A.C., R.T.B., S.C.K., R.N., D.E.H., S.W.L., and J.P. analyzed data; and J.R.M., S.W.L., and J.P. wrote the paper.

The authors declare no conflict of interest.

[‡‡]To whom correspondence may be addressed. E-mail: dhousman@mit.edu or jerry.pelletier@mcgill.ca.

This article contains supporting information online at www.pnas.org/cgi/content/full/0804821105/DCSupplemental.

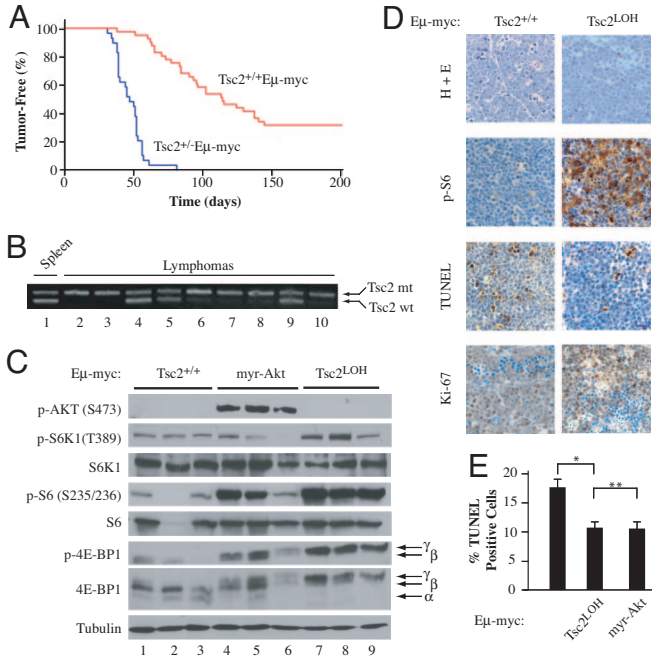

Fig. 1. *Tsc2^{LOH}Eμ-myc* tumors display accelerated lymphomagenesis and activated mTORC1 signaling. (*A*) Kaplan–Meier plot illustrating differences in tumor latencies between *Tsc2$^{+/+}$Eμ-myc* (red, $n = 41$) and *Tsc2$^{+/-}$Eμ-myc* (blue, $n = 29$) mice ($P < 0.001$ as determined by log rank analysis). (*B*) PCR to detect LOH at the *Tsc2* locus in *Tsc2$^{+/-}$Eμ-myc* tumors (wt, wild-type allele; mt, mutant allele). (*C*) Western blot analysis of *Eμ-myc* tumors of the indicated genotypes probed for activation of AKT-mTOR signaling (*p*-AKT, α-tubulin, and phosphorylated and total S6K1, S6, and 4E-BP1). (*D*) Representative micrographs of *Tsc2$^{+/+}$Eμ-myc* and *Tsc2^{LOH}Eμ-myc* tumor sections stained with H&E, by TUNEL, and for Ki-67. (*E*) Loss of TSC2 blocks MYC-induced apoptosis to the same extent as AKT activation. The percentage of cells staining positive for TUNEL from *Tsc2$^{+/+}$Eμ-myc* ($n = 4$), *Tsc2^{LOH}Eμ-myc* ($n = 3$), or *Eμ-myc*/myr-*Akt* ($n = 3$) tumors is shown. Tumor tissue sections from three independent animals were analyzed, with three randomly selected fields (≈500 cells) analyzed for TUNEL signal. Error bars represent the SD. *, $P < 0.001$; **, $P \approx 0.4$ as determined by Student's *t* test.

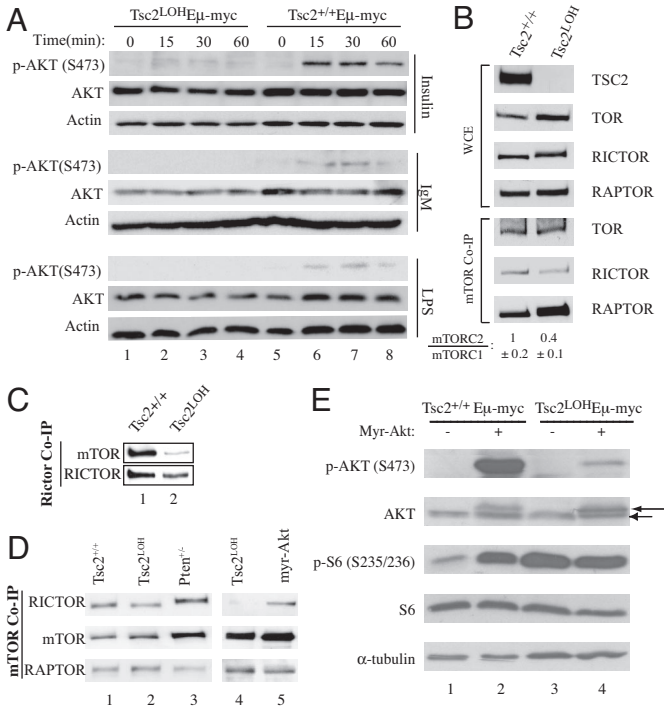

Fig. 2. Activation of mTORC1 leads to defective AKT phosphorylation in MYC-induced lymphomagenesis. (*A*) Tumors of the indicated genotype were cultured *ex vivo* and stimulated with 100 nM insulin, 10 μg/ml LPS, or 10 μg/ml IgM. Extracts were prepared and probed for AKT (total and *p*-S473) and ACTIN. (*B*) The distribution of mTOR among mTORC1 and mTORC2 is altered in *Tsc2^{LOH}Eμ-myc* tumors. *Tsc2$^{+/+}$Eμ-myc* and *Tsc2^{LOH}Eμ-myc* tumors were analyzed for total levels of mTOR, RICTOR, and RAPTOR. MTOR-containing complexes were immunoprecipitated from *Eμ-myc* tumors of the indicated genotypes, and RICTOR and RAPTOR levels were assessed by Western blotting. (*Top*) Total levels of mTOR, RICTOR, and RAPTOR in whole-cell extracts. (*Bottom*) Amounts of RICTOR and RAPTOR coprecipitating (Co-IP) with mTOR. The quantitation of mTORC2:mTORC1 ratios in three tumors of the indicated genotype is shown and represents the average of three experiments ±SD. (*C*) *Tsc2$^{+/+}$Eμ-myc* and *Tsc2^{LOH}Eμ-myc* tumors were analyzed for levels of RICTOR-associated mTOR. (*D*) Amounts of RICTOR and RAPTOR associating with mTOR in *Eμ-myc*, *Tsc2^{LOH}*, *myr-Akt*, and *Pten$^{+/-}$Eμ-myc* tumors. (*E*) AKT (S473) phosphorylation is decreased in *Tsc2^{LOH}Eμ-myc* tumors. Extracts prepared from MSCV/myr-*Akt*-infected *Tsc2$^{+/+}$Eμ-myc* or *Tsc2^{LOH}Eμ-myc* tumors were analyzed by Western blotting for AKT (total and *p*-S473), S6 (total and *p*-S235/236), and tubulin. AKT and myr-AKT are denoted by an arrow and arrowhead, respectively.

this work as *Tsc2^{LOH}Eμ-Myc*), as judged by phosphorylation of S6K1 and 4E-BP1 (Fig. 1*C*; lanes 7–9). 4E-BP1 and S6K1 phosphorylation were elevated in *Eμ-Myc*/myr-*Akt* tumors although not as extensively (lanes 4–6). Tumors lacking lesions in the AKT/mTORC1 pathway showed little phosphorylation of rpS6, S6K1, and 4E-BP1 (lanes 1–3). Taken together, the results indicate robust mTORC1 activation in *Tsc2^{LOH}Eμ-Myc* tumors.

Forced activation of AKT in the context of the *Eμ-Myc* mouse model results in tumors that show little change in proliferation rates but have suppressed apoptosis (8). Immunohistochemical (IHC) analysis confirmed that both tumor genotypes showed similar levels of proliferation as revealed by Ki67 staining; however, *Tsc2^{LOH}Eμ-Myc* tumors had reduced apoptotic rates, similar to what was observed in AKT-driven tumors (Fig. 1 *D* and *E*). IHC also verified that mTORC1 was active because there was elevated *p*-S6 staining in *Tsc2^{LOH}Eμ-Myc* tumors compared with *Tsc2$^{+/+}$Eμ-Myc* tumors (Fig. 1*D*). This is consistent with activated mTORC1 regulating programmed cell death in the *Eμ-Myc* mouse model (8). The impact of *Tsc2* loss on tumor behavior was reminiscent of AKT-driven lymphomas because *Tsc2^{LOH}Eμ-Myc* tumors maintained functional p53, whereas E*μ-Myc* commonly do not (12). p53 alleles were intact and lacked any mutations as determined by sequencing of all 11 p53 exons from a panel of 11 *Tsc2^{LOH}Eμ-Myc* tumors (data not shown). *Tsc2^{LOH}Eμ-Myc* tumors retained p53 protein expression and repressed ARF expression (Fig. S2*A*). Detection of exon 1β of *Arf* verified the presence of the *Arf* locus (Fig. S2*B*), and *Tsc2^{LOH}Eμ-Myc* tumors responded appropriately to γ-irradiation by up-regulating p53 and p21 expression (Fig. S2*C*). Knockdown of p53 in *Tsc2^{LOH}Eμ-Myc* tumors blocked induction of p21, whereas p53$^{-/-}$*Eμ-Myc* tumors failed to activate p21 (Fig. S2*C*). Thus, *Tsc2^{LOH}Eμ-Myc* tumors retained a functional p53 pathway.

***Tsc2^{LOH}Eμ-Myc* Lymphomas Have Defective AKT Activation.** Loss of TSC2 in mouse embryonic fibroblasts (MEFs) impairs AKT activation by blocking PI3K-dependent recruitment to the membrane, where it is fully activated by phosphorylation on S473 by mTORC2 (13, 14). We tested the inducibility of AKT in *Tsc2^{LOH}Eμ-Myc* tumors by measuring S473 phosphorylation after treatment with various PI3K stimulators (Fig. 2*A*). Insulin, LPS, and IgM were incapable of eliciting AKT (S473) phosphorylation in *Tsc2^{LOH}Eμ-Myc* tumors (lanes 1–4). In contrast, *Tsc2$^{+/+}$Eμ-Myc* tumors were responsive to these stimuli (lanes 5–8).

Another important consequence of loss of TSC2 is an alteration in the distribution of mTOR among its complexes, mTORC1 and mTORC2 (15). Loss of mTORC2 has been shown to stimulate mTORC1 signaling (16). We therefore measured the proportion

of mTOR present in mTORC1 (associating with RAPTOR) or mTORC2 (associating with RICTOR) in *Tsc2*^{LOH}*Eμ-Myc* and *Tsc2*$^{+/+}$*Eμ-Myc* tumors (Fig. 2*B*). Anti-mTOR antibodies immunoprecipitated less RICTOR from *Tsc2*^{LOH}*Eμ-Myc* lymphomas compared with *Tsc2*$^{+/+}$*Eμ-Myc* lymphomas (Fig. 2*B*; ≈2.5-fold decrease). Similarly, anti-RICTOR antibodies immunoprecipitated less mTOR in *Tsc2*^{LOH}*Eμ-Myc* tumors (Fig. 2*C*). *Tsc2*$^{-/-}$*p53*$^{-/-}$ MEFs had similar changes in mTORC1 and mTORC2 levels compared with *Tsc2*$^{+/+}$*p53*$^{-/-}$ MEFs (Fig. S3). We also analyzed mTOR complexes in *Pten*$^{+/-}$*Eμ-Myc* and *Eμ-Myc/myr-Akt* tumors and did not find significant changes in mTORC2:mTORC1 ratios compared with *Eμ-Myc* tumors (Fig. 2*D*, compare lanes 3 and 5 with 1). Loss of mTORC2 complexes could explain why we noted only weak phosphorylation of constitutively membrane recruited myr-AKT in *Tsc2*^{LOH}*Eμ-Myc* tumors (Fig. 2*E*). Hence, despite loss of AKT activation, *Tsc2*^{LOH}*Eμ-Myc* tumors develop rapidly with a suppressed apoptotic program.

mTORC1 Mediates Cell Survival in *Tsc2*^{LOH}*Eμ-Myc* Lymphomas. *Tsc2*^{LOH}*Eμ-Myc* derived tumors had significantly lower levels of apoptosis (Fig. 1*E*), prompting us to assess their drug sensitivity. C57BL/6 mice bearing transplanted primary *Tsc2*^{LOH}*Eμ-Myc* lymphomas were treated with either doxorubicin (*Dxr*), rapamycin (*Rap*), or combination therapy (*Dxr* + *Rap*) and monitored for tumor-free survival. Here, animals bearing *Arf*$^{-/-}$*Eμ-myc* lymphomas were used as controls because these lymphomas are also highly aggressive but remain chemosensitive (8, 17). Mice bearing control tumors underwent complete remission for ≈18 days after *Dxr* treatment (data not shown) as reported in ref. 8. Mice bearing *Tsc2*^{LOH}*Eμ-Myc* lymphomas showed little response to *Dxr*, with tumors relapsing by 5 days after treatment (Fig. 3*A*; $P < 0.001$ relative to control lymphomas). Mice bearing control lymphomas did not respond to *Rap* (data not shown), whereas mice harboring *Tsc2*^{LOH}*Eμ-Myc* lymphomas showed complete remission for ≈10 days after *Rap* therapy (Fig. 3*A*; medium dash, $P < 0.001$ compared with control lymphomas). *Tsc2*^{LOH}*Eμ-Myc* lymphomas were highly sensitive to the combination of *Rap* and *Dxr*, similar to what has been observed for *Eμ-Myc/myr-Akt*- derived lymphomas (Fig. 3*A*; $P < 0.001$ compared with single agents). This enhanced sensitivity was associated with increased apoptosis as assessed by PARP cleavage (Fig. 3*B*). *Tsc2*^{LOH}*Eμ-Myc* tumors rapidly underwent apoptosis after a single dose of *Rap in vivo* (Fig. 3*B* and Fig. S4 *A* and *B*). *Arf*$^{-/-}$*Eμ-myc* or *Eμ-Myc* tumors were both unresponsive to five consecutive daily doses of *Rap in vivo* (data not shown). These differences were recapitulated *ex vivo* (Fig. 3 *C* and *D*).

An *in vitro* competition assay revealed that shRNAs directed against RAPTOR were selected against whether *Rap* was present or not, whereas decreasing RICTOR had no influence on *Rap* sensitivity (Fig. 3*E*). shRNA directed against eIF4E, a downstream effector of mTORC1, proved to be moderately selected against under normal growth conditions; however, in the presence of *Rap*, eIF4E shRNA-expressing tumors were eliminated from the population. Taken together, our results suggest that mTORC1 mediates survival signaling in *Tsc2*^{LOH}*Eμ-Myc* lymphomas.

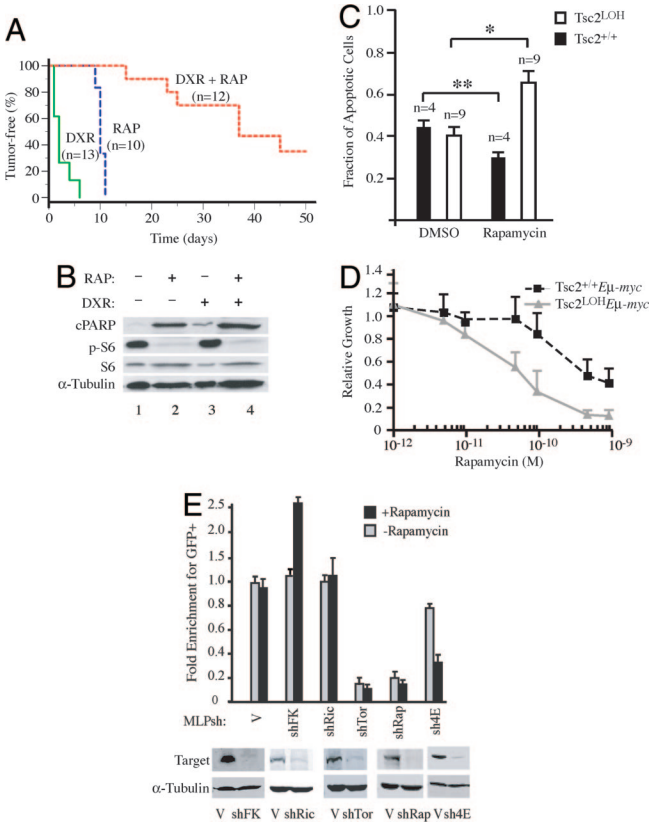

Fig. 3. Rapamycin and doxorubicin cooperatively induce apoptosis in *Tsc2*^{LOH}*Eμ-myc* tumors. (*A*) Kaplan–Meier plot detailing the time to relapse after treatment of mice bearing *Tsc2*^{LOH}*Eμ-Myc* tumors with *Dxr*, *Rap*, or a combination of both (*Dxr* + *Rap*). $P < 0.001$ for significance among all curves as determined by log rank test. (*B*) Extracts prepared from *Tsc2*^{LOH}*Eμ-myc* tumors treated with *Rap*, *Dxr*, or combination treatment were probed for cleaved PARP (cPARP), tubulin, and rpS6 (S6 and *p*-S235/236). (*C*) *Tsc2*^{LOH}*Eμ-myc* tumors are more sensitive to *Rap*-induced apoptosis than *Tsc2*$^{+/+}$*Eμ-myc* tumors. *Eμ-myc* derived tumors (*Tsc2*$^{+/+}$ or *Tsc2*^{LOH}) were cultured *ex vivo* in the presence of vehicle or 1 nM *Rap* for 32 h. Propidium iodide and annexin V staining was used to quantify induction of apoptosis. *, $P < 0.0007$; **, $P \approx 0.2$ as determined by Student's *t* test. (*D*) *Tsc2*^{LOH}*Eμ-myc* tumors are more sensitive to growth inhibition than *Tsc2*$^{+/+}$*Eμ-myc* tumors. Cells were cultured *ex vivo* in the presence of the indicated concentrations of *Rap* for 24 h and viability determined by using an MTS assay (Promega). Viability is standardized to nontreated controls ($n = 3$). (*E*) mTORC1, not mTORC2, dictates sensitivity to *Rap* in *Tsc2*^{LOH}*Eμ-myc* lymphomas. (*Upper*) *Tsc2*^{LOH}*Eμ-myc* lymphomas were cultured *ex vivo* and transduced with the indicated MLP-based shRNA vectors. The percentage viable GFP$^+$ cells was measured after a 60-h exposure to 50 pM rapamycin or vehicle alone. The results are expressed relative to percentage GFP$^+$ cells present before rapamycin exposure (which was arbitrarily set at 1). Shown are averaged over three experiments, and error bars represent the SEM. (*Lower*) Immunoblots verifying knockdown of target proteins using the indicated MSCV-based shRNA retroviral vectors in NIH 3T3 cells.

***Mcl-1* Translation Is mTORC1-Regulated.** Activation of mTORC1 is predicted to stimulate protein synthesis (2). Indeed, *Eμ-Myc* tumors lacking TSC2 showed a 2-fold increase in protein synthetic rates compared with *Tsc2*$^{+/+}$*Eμ-Myc* tumors (Fig. 4*A*). This increased translation is mTORC1-dependent because *Rap* inhibited translation to levels comparable with those observed in *Tsc2*$^{+/+}$*Eμ-Myc* tumors (Fig. 4*A*). Similar results were obtained with *Tsc2*$^{-/-}$*p53*$^{-/-}$ and *Tsc2*$^{+/+}$*p53*$^{-/-}$ MEFs (Fig. S5*A*). To determine whether the *Rap*-mediated decreases in translation were associated with altered levels of eIF4F complex, we measured the relative levels of eIF4E-binding partners, eIF4GI and 4E-BP1, associating with cap-bound eIF4E (Fig. 4*B*). As expected, the amount of eIF4G associating with eIF4E was reduced, whereas the amount of inhibitory 4E-BP1 increased in *Rap*-treated samples (compare lane 4 with 3). Thus, *Rap* reduces eIF4F complexes in *Tsc2*^{LOH}*Eμ-Myc* tumors, and this correlates with a decrease in translation rates.

Given that mTORC1 inhibition in *Tsc2*^{LOH}*Eμ-Myc* lymphomas leads to a rapid onset of apoptosis, we postulated that activated mTORC1 was promoting drug resistance by increasing the translation of antiapoptotic proteins. Unlike other antiapoptotic *bcl-2*-like family members, MCL-1 is a highly unstable protein and requires active translation to maintain its expression levels (18). MCL-1 is necessary for early embryonic development and for maintenance of hematopoietic cell lineages (19). In the *Eμ-Myc* mouse model, eIF4E has been shown to regulate MCL-1 expression (20). Indeed, we observed modest but consistent increases

GENETICS

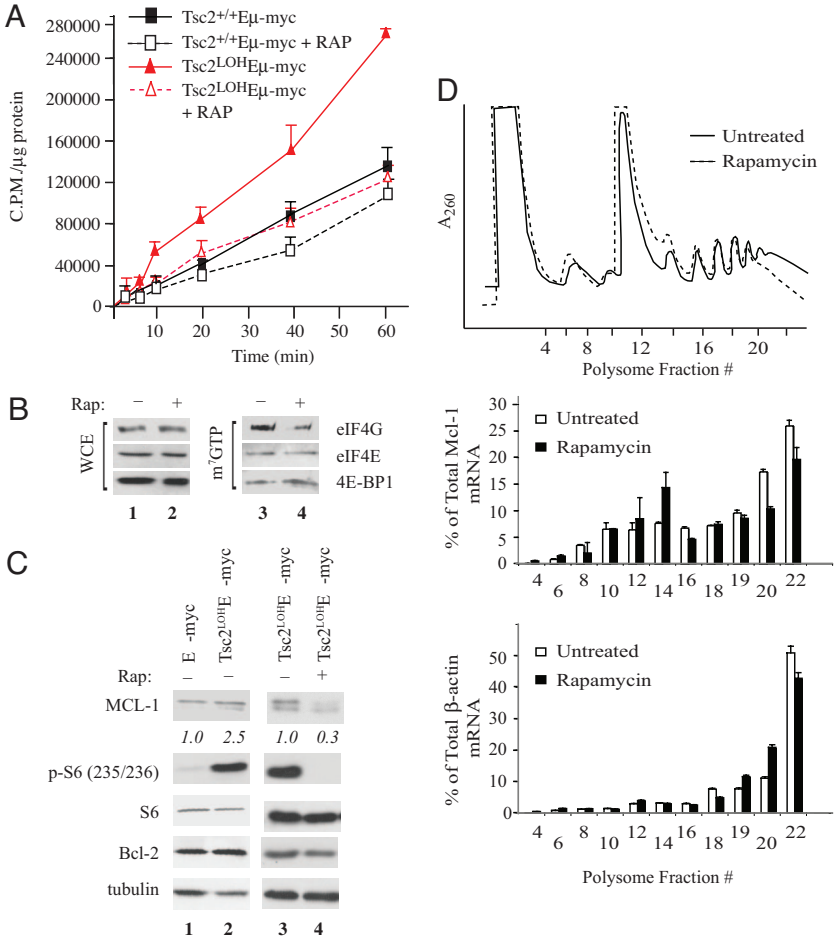

Fig. 4. Rapamycin decreases expression of MCL-1 in *Tsc2^{LOH}Eμ-myc* tumors. (*A*) *Eμ-myc*-derived tumors (*Tsc2$^{+/+}$* or *Tsc2^{LOH}*) were cultured *ex vivo* in the presence of vehicle or 10 nM *Rap* for 2 h followed by [^{35}S]Met labeling for the indicated times. Error bars represent SD (n = 2). (*B*) *Rap* treatment of *Tsc2^{LOH}Eμ-myc* tumors impairs recruitment of eIF4GI into the eIF4F complex. Extracts from *Tsc2^{LOH}Eμ-myc* and *Tsc2$^{+/+}$Eμ-myc* tumors were applied to m^{7}GDP affinity resins and washed, and m^{7}GTP eluents were probed for eIF4GI, eIF4E, and 4E-BP1. (*C*) Expression of *Mcl-1* is mTOR-dependent in *Tsc2^{LOH}Eμ-myc* cells. After 1 h of *Rap* treatment, MCL-1 levels were determined by Western blotting. (*D*) Translation of *Mcl-1* is inhibited by Rap. Polysome profiles from *Tsc2^{LOH}Eμ-myc* tumors grown *ex vivo* and exposed to 10 nM *Rap* for 2 h are shown. RNA was isolated from polysome fractions and subjected to quantitative RT-PCR analysis. The relative amount of *Mcl-1* or *β-actin* mRNA in each fraction is expressed as a percentage of the total in the polysome gradient. Quantitative RT-PCRs were performed in duplicate, and the error bars represent the SEM. Shown is one of three representative experiments performed on different polysome gradients.

in MCL-1 expression in *Tsc2^{LOH}Eμ-Myc* tumors compared with *Eμ-Myc* tumors (Fig. 4*C*) and in *Tsc2$^{-/-}$p53$^{-/-}$* MEFs compared with *Tsc2$^{+/+}$p53$^{-/-}$* MEFs under low serum conditions (Fig. S5*B*). Rescue of TSC2 expression in *Tsc2$^{-/-}$p53$^{-/-}$* MEFs reduced MCL-1 to levels observed in *Tsc2$^{+/+}$p53$^{-/-}$* MEFs (Fig. S5*B*). Inhibition of mTORC1 by *Rap* reduced MCL-1 to basal levels in both *Tsc2^{LOH}Eμ-Myc* tumors and *Tsc2$^{-/-}$p53$^{-/-}$* MEFs (Fig. 4*C* and Fig. S5 *B* and *C*). Interestingly, in both lymphomas and MEFs lacking a lesion activating mTORC1 signaling, *Rap* neither induced apoptosis nor appreciably decreased MCL-1 expression (Fig. S5 *B* and *C*). Hence, loss of MCL-1 expression by mTORC1 inhibition occurs in the context of activated AKT/mTORC1 signaling.

To determine whether this was a consequence of a decrease in *Mcl-1* translation, we monitored the polysome distribution of *Mcl-1* in untreated or *Rap*-treated *Tsc2^{LOH}Eμ-Myc* tumors (Fig. 4*D*). *Rap* treatment of *Tsc2^{LOH}Eμ-Myc* tumors produced a depression in the distribution of heavy polysomes and increased the amount of lighter polysomes and free ribosomes (Fig. 4*D*). Quantitative RT-PCR revealed a redistribution of *Mcl-1* mRNA from heavy polysomes (fraction 20–22) in *Rap*-treated cells toward lighter polysomes (fraction 12–14). This contrasts with the behavior of *β-actin* mRNA from the same polysome fractions, which showed only slight differences in distribution between untreated and *Rap*-treated samples (Fig. 4*D*).

Rapamycin-Induced Apoptosis Is Rescued by MCL-1 Overexpression. These findings raised the question of whether *Rap*-induced apoptosis in *Tsc2^{LOH}Eμ-Myc* tumors was initiated by the loss of *Mcl-1* expression. To address this, we established an *in vivo* competition assay that allowed us to generate genetically defined mixed tumor populations and examine relative competitiveness of each population *in vivo* (Fig. 5*A*). *Tsc2^{LOH}Eμ-Myc* tumors were freshly isolated from donors and partially infected with either MSCV/*gfp* or MSCV/*Mcl-1*/*gfp*. These populations were reintroduced into recipient syngenic animals, and upon tumor manifestation, the mice received either vehicle or *Rap*. Before therapy, mice were visualized to detect GFP$^+$ tumors in the abdominal region. At 12 h after *Rap*, the time required to detect appreciable loss of tumor mass in *Tsc2^{LOH}Eμ-Myc* mice, the same mice were again visualized to quantitate the amount of GFP$^+$ tumor cells (Fig. 5*B*). *Rap* treatment led to a detectable decrease in the tumor size and correlated with a loss of GFP signal intensity (Fig. 5*B Left pair*). In contrast, an increase in GFP intensity was observed in mice bearing *Tsc2^{LOH}Eμ-Myc* tumors infected with MSCV/*Mcl-1*/*gfp* (Fig. 5*B Right pair*). The amount of GFP$^+$ cells was quantitated by harvesting the residual tumor cells and subjecting these to flow cytometry (Fig. 5*C*). Enrichment of GFP$^+$ cells after Rap therapy is clearly seen in MSCV/*Mcl-1*/gfp-infected cells and indicates resistance to therapy. Thus, *Mcl-1* is a genetic modifier of Rap sensitivity.

Discussion

Here, we established that mTORC1 acts as a key mediator of AKT prosurvival functions in B cell lymphomas driven by MYC overexpression. *Tsc2$^{+/-}$Eμ-Myc* mice rapidly developed aggressive lymphomas with tumors frequently undergoing LOH (Fig. 1 *A* and *B*), an event associated with hyperactive mTORC1 signaling (Fig. 1*C*). The c-*myc* oncogene promotes apoptosis, such that genetic alterations that disable apoptotic programs often accelerate *MYC*-driven tumorigenesis (21). Not surprisingly, *Tsc2^{LOH}Eμ-Myc* lymphomas arose with defective apoptotic responses to oncogene

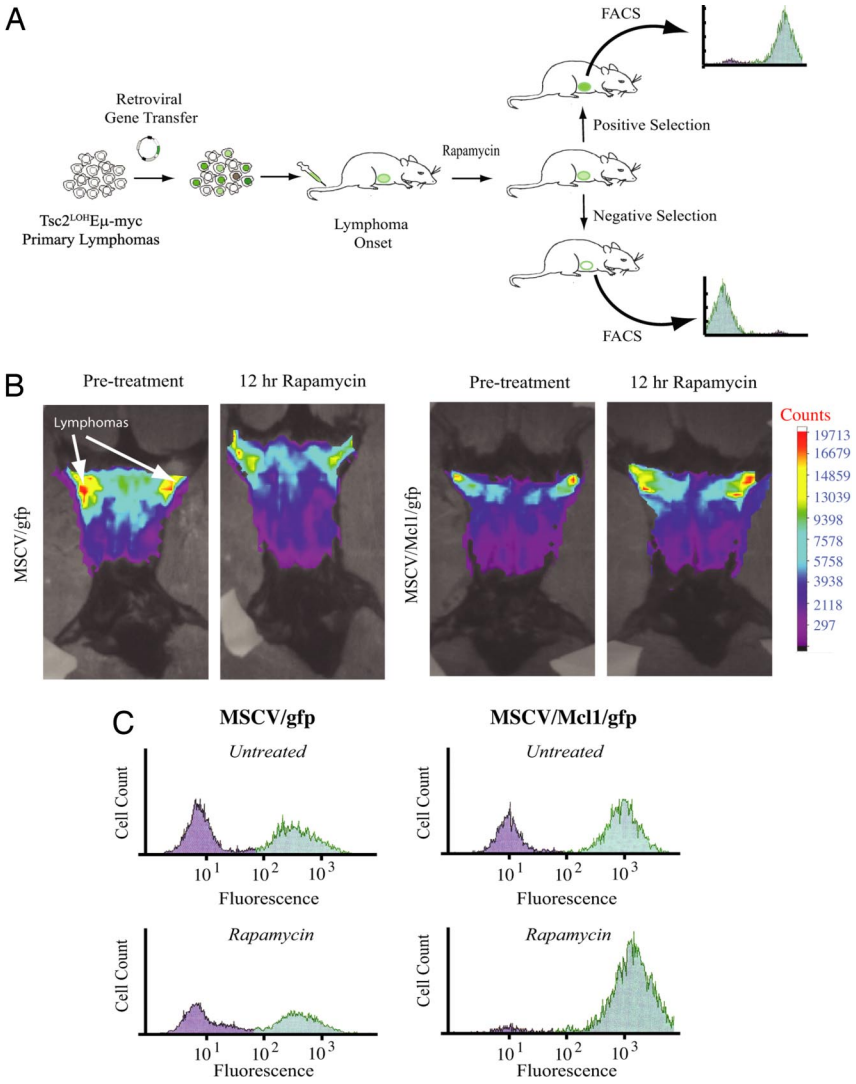

Fig. 5. *Mcl-1* is a genetic modifier of rapamycin sensitivity *in vivo*. (*A*) Schematic representation of the *in vivo* competition experimental design. (*B*) Freshly isolated $Tsc2^{LOH}E\mu$-*myc* tumors were transduced *ex vivo* with MSCV/*gfp* or MSCV/*Mcl-1*/gfp virus and introduced into syngenic mice. Upon tumor formation, the GFP content of tumors was determined by fluorescence whole-body scanning with the GE eXplore Optix. The fluorescence signal in each animal was analyzed before and 12 h after a single dose of *Rap*. The intensity of the GFP signal is depicted by color according the bar scale at the right. (*C*) Representative flow cytometry analysis of GFP expression in $Tsc2^{LOH}E\mu$-*myc* tumors expressing *gfp* and *Mcl-1* in the viable portion of tumors harvested 12 h after *Rap* exposure.

activation and chemotherapy. These defects were reversible upon mTORC1 inhibition. We reported that tumors in $Pten^{+/-}E\mu$-*Myc* mice arise at a rate comparable to $E\mu$-*Myc* mice. Interestingly, $Pten^{+/-}E\mu$-*Myc* did not undergo LOH, nor did they arise with robust activation of mTORC1 as seen in $E\mu$-*Myc*/*myr-Akt* lymphomas or $Tsc2^{LOH}E\mu$-*Myc* lymphomas (8). These findings highlight the importance of mTORC1 activity as a potent antiapoptotic signal and as a critical arm of AKT-driven tumorigenesis in lymphoma development.

One mechanism by which mTORC1 activity can promote cell survival is through increased availability of eIF4E for assembly into the eIF4F, a rate-limiting complex required for the ribosome recruitment phase of translation initiation (2, 22). Increased eIF4E levels can effectively suppress c-*myc*-induced apoptosis *in vivo* and alter chemosensitivity *in vivo* (8). We hypothesized that a sizeable proportion of AKT survival signaling may result from deregulated translation, perhaps through altering the recruitment of antiapoptotic mRNAs to the translation apparatus (7, 8, 20). We find that $Tsc2^{LOH}E\mu$-*Myc* lymphomas have ≈2-fold higher translation rates than $Tsc2^{+/+}E\mu$-*Myc* lymphomas (Fig. 4*A*). mTORC1 inhibition reduced translation rates to levels that resembled those observed in $Tsc2^{+/+}E\mu$-*Myc* cells and decreased eIF4F levels (Fig. 4 *A* and *B*). In contrast, translation rates in $E\mu$-*Myc* tumors were minimally affected by *Rap*, consistent with the absence of mTORC1 activation in these tumors (Fig. 4*A*). By using an *in vitro* competition assay with shRNAs targeting components of mTOR signaling complexes, we determined that the sensitivity to rapamycin was indeed mediated through the mTORC1/eIF4E arm (Fig. 3*E* and data not shown). Higher eIF4E levels preferentially increase the translation of mRNAs having lengthy, G+C-rich, highly structured 5′ UTRs and drive cellular transformation and metastatic progression in preclinical models (22). In this fashion, the translation of "weak" mRNAs is preferentially affected when eIF4F levels are modulated by mTORC1 (22, 23). Hence, treatment of $Tsc2^{LOH}E\mu$-*Myc* tumor cells with rapamycin may reflect translation inhibition of weak mRNAs (Fig. 4*A*).

One such mRNA is *Mcl-1*, which has a G+C-rich (>70%) 5′ UTR (see NM_021960). MCL-1 is a short-lived protein with a complex mode of regulation. Our previous studies and work by others have implicated MCL-1 as a potential downstream target of eIF4E (20, 24, 25). Elimination of MCL-1 is required for the initiation of apoptosis after UV irradiation. During DNA damage, *Mcl-1* protein synthesis is blocked, and the existing pool of MCL-1 is rapidly degraded by the proteasome (18). Inhibition of *Mcl-1* expression is effective at inducing apoptosis in some human cancers (26, 27). We demonstrate that *Rap* caused a decrease in MCL-1 levels in $Tsc2^{LOH}E\mu$-*Myc* tumors. This response is associated with a decrease in the translational efficiency of the *Mcl-1* mRNA (Fig. 4 *C* and *D*) and induction of apoptosis (Fig. 3 *B* and *D* and Fig. S4 *A* and *B*). Consistent with deregulated *Mcl*-1 expression modulating

drug sensitivity, constitutive expression of *Mcl-1* in $Tsc2^{LOH}E\mu$-*Myc* cells prevented tumor regression upon mTORC1 inhibition (Fig. 5). Our results do not exclude the possibility that additional levels of *Mcl-1* regulation contribute to the effects reported herein, but they do indicate that *Mcl-1* mRNA translation is an important target of rapamycin *in vivo*. Tumors arising with activating lesions in the AKT pathway often display *Rap* sensitivity. Interestingly, we find that *Rap* only inhibits *Mcl-1* expression in the context of activating lesions in the AKT/mTORC1 pathway (Fig. S4*C*). In lymphomas, lacking activation of this pathway, *Rap* does not induce tumor regression, nor does it reduce expression of *Mcl-1*. Our findings highlight the importance of mTORC1 activity as a potent antiapoptotic signal through *Mcl-1* and as a critical arm of PI3K/AKT-driven tumorigenesis in lymphoma development.

Materials and Methods

Immunblotting. For immunoblots, 50 μg of protein extract was typically loaded per lane and electrophoretically separated on SDS/polyacrylamide gels. Proteins were transferred to Immobilon-P membranes (Millipore). Specific proteins were detected with antibodies listed in the *SI Materials and Methods*.

***In Vivo* Tumor Monitoring.** Tumors were analyzed for gfp expression by using the GE eXplore Optix system (GE Healthcare) with a 470-nm emitting laser. Photon emission counts were collected and converted to GFP signal intensity. Mice bearing tumors were analyzed before and 12 h after Rap therapy.

Tumor Analyses. For generating whole-cell protein extracts, tumors were harvested, and single cell suspensions were made. These cells were treated with ACK buffer [0.15 M NH_4Cl, 0.1 mM EDTA, 0.01 M $KHCO_3$ (pH 7.3)] to remove red blood cells. Cells were pelleted, washed several times with ice-cold PBS, and resuspended in ice-cold lysis buffer [10 mM Tris·HCl (pH 7.6), 1% Nonidet P-40, 0.5% sodium desoxycholate, 0.1% SDS, 20 mM β-glycerophosphate, 10 mM NaF, 100 mM NaCl, 1 mM EDTA, 1 mM EGTA, 1 μg/ml pepstatin, 1 μg/ml leupeptin, and 1 μg/ml aprotinin] and left on ice for 15 min. The resulting lysates were then sonicated on ice for 10 s, and debris was pelleted by centrifugation at 14,000 $\times$ *g* for 15 min at 4°C. The resulting supernatant was quantitated for protein concentration and frozen at −80°C.

Coimmunoprecipitations. mTOR and RICTOR coimmunprecipitations were performed according to published methods (28) with slight modifications, described in *SI Materials and Methods*.

Polysome Analysis and Real-Time Quantitative RT-PCR. For polysome profiling, $Tsc2^{LOH}E\mu$-*myc* lymphomas were treated for 2 h with vehicle (MeOH) or 4.0 mg/kg Rap. Cells were then processed for polysome analysis as described in *SI Materials and Methods*.

ACKNOWLEDGMENTS. We thank Dr. David Kwiatkowski (Brigham and Women's Hospital, Boston, MA) for supplying $Tsc2^{-/-p53-/-}$ and $Tsc2^{+/+p53-/-}$ MEFs. We thank Yifei Yan for statistical evaluations, Isabelle Harvey for assistance with the mouse colony, and Kris Pike and Dr. David Munroe for p53 gene sequencing. This work was supported by Canadian Breast Cancer Research Alliance Translational Acceleration Grant 16512 and Canadian Institutes of Health Research Grant MOP-79385 (to J.P.) and National Cancer Institute/National Institutes of Health Grant CA87497 (to S.W.L.).

1. Guertin DA, Sabatini DM (2007) Defining the role of mTOR in cancer. *Cancer Cell* 12:9–22.
2. Hay N, Sonenberg N (2004) Upstream and downstream of mTOR. *Genes Dev* 18:1926–1945.
3. Dorrello NV, *et al*. (2006) S6K1- and β-TRCP-mediated degradation of PDCD4 promotes protein translation and cell growth. *Science* 314:467–471.
4. Lopiccolo J, Blumenthal GM, Bernstein WB, Dennis PA (2008) Targeting the PI3K/Akt/mTOR pathway: Effective combinations and clinical considerations. *Drug Resist Update* 11:32–50.
5. Sarbassov DD, *et al*. (2006) Prolonged rapamycin treatment inhibits mTORC2 assembly and Akt/PKB. *Mol Cell* 22:159–168.
6. O'Reilly KE, *et al*. (2006) mTOR inhibition induces upstream receptor tyrosine kinase signaling and activates Akt. *Cancer Res* 66:1500–1508.
7. Wendel HG, *et al*. (2006) Determinants of sensitivity and resistance to rapamycin-chemotherapy drug combinations *in vivo*. *Cancer Res* 66:7639–7646.
8. Wendel HG, *et al*. (2004) Survival signalling by Akt and eIF4E in oncogenesis and cancer therapy. *Nature* 428:332–337.
9. Skeen JE, *et al*. (2006) Akt deficiency impairs normal cell proliferation and suppresses oncogenesis in a p53-independent and mTORC1-dependent manner. *Cancer Cell* 10:269–280.
10. Zhang H, *et al*. (2003) Loss of Tsc1/Tsc2 activates mTOR and disrupts PI3K-Akt signaling through down-regulation of PDGFR. *J Clin Invest* 112:1223–1233.
11. Adams JM, *et al*. (1985) The c-*myc* oncogene driven by immunoglobulin enhancers induces lymphoid malignancy in transgenic mice. *Nature* 318:533–538.
12. Eischen CM, Weber JD, Roussel MF, Sherr CJ, Cleveland JL (1999) Disruption of the ARF-Mdm2–p53 tumor suppressor pathway in Myc-induced lymphomagenesis. *Genes Dev* 13:2658–2669.
13. Harrington LS, *et al*. (2004) The TSC1–2 tumor suppressor controls insulin-PI3K signaling via regulation of IRS proteins. *J Cell Biol* 166:213–223.
14. Guertin DA, *et al*. (2006) Ablation in mice of the mTORC components raptor, rictor, or mLST8 reveals that mTORC2 is required for signaling to Akt-FOXO and PKCα, but not S6K1. *Dev Cell* 11:859–871.
15. Schieke SM, *et al*. (2006) The mammalian target of rapamycin (mTOR) pathway regulates mitochondrial oxygen consumption and oxidative capacity. *J Biol Chem* 281:27643–27652.
16. Sarbassov DD, Guertin DA, Ali SM, Sabatini DM (2005) Phosphorylation and regulation of Akt/PKB by the rictor-mTOR complex. *Science* 307:1098–1101.
17. Schmitt CA, McCurrach ME, de Stanchina E, Wallace-Brodeur RR, Lowe SW (1999) INK4a/ARF mutations accelerate lymphomagenesis and promote chemoresistance by disabling p53. *Genes Dev* 13:2670–2677.
18. Nijhawan D, *et al*. (2003) Elimination of Mcl-1 is required for the initiation of apoptosis following ultraviolet irradiation. *Genes Dev* 17:1475–1486.
19. Opferman JT, *et al*. (2003) Development and maintenance of B and T lymphocytes requires antiapoptotic MCL-1. *Nature* 426:671–676.
20. Wendel HG, *et al*. (2007) Dissecting eIF4E action in tumorigenesis. *Genes Dev* 21:3232–3237.
21. Hemann MT, *et al*. (2005) Evasion of the p53 tumour surveillance network by tumour-derived MYC mutants. *Nature* 436:807–811.
22. Graff JR, Konicek BW, Carter JH, Marcusson EG (2008) Targeting the eukaryotic translation initiation factor 4E for cancer therapy. *Cancer Res* 68:631–634.
23. Dever TE (2002) Gene-specific regulation by general translation factors. *Cell* 108:545–556.
24. Vega F, *et al*. (2006) Activation of mammalian target of rapamycin signaling pathway contributes to tumor cell survival in anaplastic lymphoma kinase-positive anaplastic large cell lymphoma. *Cancer Res* 66:6589–6597.
25. Wei G, *et al*. (2006) Gene expression-based chemical genomics identifies rapamycin as a modulator of MCL1 and glucocorticoid resistance. *Cancer Cell* 10:331–342.
26. Wuilleme-Toumi S, *et al*. (2005) Mcl-1 is overexpressed in multiple myeloma and associated with relapse and shorter survival. *Leukemia* 19:1248–1252.
27. Podar K, *et al*. (2008) A pivotal role for Mcl-1 in Bortezomib-induced apoptosis. *Oncogene* 27:721–731.
28. Sarbassov DD, *et al*. (2004) Rictor, a novel binding partner of mTOR, defines a rapamycin-insensitive and raptor-independent pathway that regulates the cytoskeleton. *Curr Biol* 14:1296–1302.